

Dynamic parabolic pulse generation using temporal shaping of wavelength to time mapped pulses

Dat Nguyen,^{1,2} Mohammad Umar Piracha,¹ Dimitrios Mandridis,¹ and Peter J. Delfyett^{1,3}

¹CREOL, The College of Optics and Photonics, University of Central Florida, Orlando, Florida 32816, USA

²dtnguyen@creol.ucf.edu

³delfyett@creol.ucf.edu

Abstract: Self-phase modulation in fiber amplifiers can significantly degrade the quality of compressed pulses in chirped pulse amplification systems. Parabolic pulses with linear frequency chirp are suitable for suppressing nonlinearities, and to achieve high peak power pulses after compression. In this paper, we present an active time domain technique to generate parabolic pulses for chirped pulse amplification applications. Pulses from a mode-locked laser are temporally stretched and launched into an amplitude modulator, where the drive voltage is designed using the spectral shape of the input pulse and the transfer function of the modulator, resulting in the generation of parabolic pulses. Experimental results of pulse shaping with a pulse train from a mode-locked laser are presented, with a residual error of less than 5%. Moreover, an extinction ratio of 27 dB is achieved, which is ideal for chirped pulse amplification applications.

©2011 Optical Society of America

OCIS codes: (140.4050) Mode-locked lasers; (320.5540) Pulse shaping; (060.2320) Fiber optics amplifiers & oscillators; (320.7090) Ultrafast lasers.

References and links

1. D. Strickland and G. Mourou, "Compression of amplified chirped optical pulses," *Opt. Commun.* **56**(3), 219–221 (1985).
2. M. Pessot, P. Maine, and G. Mourou, "1000 times expansion/compression of optical pulses for chirped pulse amplification," *Opt. Commun.* **62**(6), 419–421 (1987).
3. F. H. Loesel, J. P. Fischer, M. H. Götz, C. Horvath, T. Juhasz, F. Noack, N. Suhm, and J. F. Bille, "Non-thermal ablation of neural tissue with femtosecond laser pulses," *Appl. Phys. B* **66**(1), 121–128 (1998).
4. C. Sauteret, D. Husson, G. Thiell, S. Seznec, S. Gary, A. Migus, and G. Mourou, "Generation of 20-TW pulses of picosecond duration using chirped-pulse amplification in a Nd:glass power chain," *Opt. Lett.* **16**(4), 238–240 (1991).
5. A. Dubietis, "Powerful femtosecond pulse generation by chirped and stretched pulse parametric amplification in BBO crystal," *Opt. Commun.* **88**(4-6), 437 (1992).
6. K. Kim, S. Lee, and P. J. Delfyett, "1.4kW high peak power generation from an all semiconductor mode-locked master oscillator power amplifier system based on eXtreme Chirped Pulse Amplification(X-CPA)," *Opt. Express* **13**(12), 4600–4606 (2005).
7. K. Kim, S. Lee, and P. J. Delfyett, "eXtreme chirped pulse amplification-beyond the fundamental energy storage limit of semiconductor optical amplifiers," *IEEE J. Sel. Top. Quantum Electron.* **12**(2), 245–254 (2006) (Invited paper).
8. D. N. Schimpf, J. Limpert, and A. Tünnermann, "Controlling the influence of SPM in fiber-based chirped-pulse amplification systems by using an actively shaped parabolic spectrum," *Opt. Express* **15**(25), 16945–16953 (2007).
9. J. van Howe, G. Zhu, and C. Xu, "Compensation of self-phase modulation in fiber-based chirped-pulse amplification systems," *Opt. Lett.* **31**(11), 1756–1758 (2006).
10. D. N. Schimpf, E. Seise, T. Eidam, J. Limpert, and A. Tünnermann, "Control of the optical Kerr effect in chirped-pulse-amplification systems using model-based phase shaping," *Opt. Lett.* **34**(24), 3788–3790 (2009).
11. V. I. Kruglov, A. C. Peacock, J. M. Dudley, and J. D. Harvey, "Self-similar propagation of high-power parabolic pulses in optical fiber amplifiers," *Opt. Lett.* **25**(24), 1753–1755 (2000).

12. S. Boscolo, S. K. Turitsyn, V. Yu. Novokshenov, and J. H. Nijhof, "Self-similar parabolic optical solitary waves," *Theor. Math. Phys.* **133**(3), 1647–1656 (2002).
13. D. Anderson, M. Desaix, M. Karlsson, M. Lisak, and M. L. Quiroga-Teixeiro, "Wave-breaking-free pulses in nonlinear-optical fibers," *J. Opt. Soc. Am. B* **10**(7), 1185 (1993).
14. M. E. Fermann, V. I. Kruglov, B. C. Thomsen, J. M. Dudley, and J. D. Harvey, "Self-similar propagation and amplification of parabolic pulses in optical fibers," *Phys. Rev. Lett.* **84**(26), 6010–6013 (2000).
15. F. Parmigiani, C. Finot, K. Mukasa, M. Ibsen, M. A. F. Roelens, P. Petropoulos, and D. J. Richardson, "Ultra-flat SPM-broadened spectra in a highly nonlinear fiber using parabolic pulses formed in a fiber Bragg grating," *Opt. Express* **14**(17), 7617–7622 (2006).
16. V. I. Kruglov, A. C. Peacock, J. D. Harvey, and J. M. Dudley, "Self-similar propagation of parabolic pulses in normal-dispersion fiber amplifiers," *J. Opt. Soc. Am. B* **19**(3), 461 (2002).
17. T. Hirooka and M. Nakazawa, "Parabolic pulse generation by use of a dispersion-decreasing fiber with normal group-velocity dispersion," *Opt. Lett.* **29**(5), 498–500 (2004).
18. B. Kibler, C. Billet, P. A. Lacourt, R. Ferrière, L. Larger, and J. M. Dudley, "Parabolic pulse generation in comb-like profiled dispersion decreasing fibre," *Electron. Lett.* **42**(17), 965–966 (2006).
19. C. Finot, G. Millot, C. Billet, and J. Dudley, "Experimental generation of parabolic pulses via Raman amplification in optical fiber," *Opt. Express* **11**(13), 1547–1552 (2003).
20. C. Finot, B. Barviau, G. Millot, A. Guryanov, A. Sysoliatin, and S. Wabnitz, "Parabolic pulse generation with active or passive dispersion decreasing optical fibers," *Opt. Express* **15**(24), 15824–15835 (2007).
21. A. Y. Plotski, A. A. Sysoliatin, A. I. Latkin, V. F. Khopin, P. Harper, J. Harrison, and S. K. Turitsyn, "Experiments on the generation of parabolic pulses in fibers with length-varying normal chromatic dispersion," *JETP Lett.* **85**(7), 319–322 (2007).
22. A. Peacock and N. Healy, "Parabolic pulse generation in tapered silicon fibers," *Opt. Lett.* **35**(11), 1780–1782 (2010).
23. A. I. Latkin, S. K. Turitsyn, and A. A. Sysoliatin, "Theory of parabolic pulse generation in tapered fiber," *Opt. Lett.* **32**(4), 331–333 (2007).
24. B. H. Kolner, "Space-time duality and the theory of temporal imaging," *IEEE J. Quantum Electron.* **30**(8), 1951–1963 (1994).
25. S. Lee, D. Mandridis, and P. J. Delfyett, "eXtreme chirped pulse oscillator operating in the nanosecond stretched pulse regime," *Opt. Express* **16**(7), 4766–4773 (2008).

1. Introduction

Chirped pulse amplification (CPA) has been widely used to achieve pulses with high energy for many applications such as radar technology or non-thermal ablation [1–5]. Increased energy per pulse can be extracted from gain media if the pulse is chirped and temporally stretched to a pulse duration longer than the storage time of the gain media [6,7]. However, in fiberized systems, when desired energy levels are in the milliJoule range, pulse amplification is limited because nonlinearities and dispersion of the gain media can cause severe pulse distortion and consequently degrade the pulse quality. As a result, advanced measures are required to mitigate the effect of nonlinearities and dispersion. Pulse shaping techniques that control amplitude and phase of input pulses have been investigated, and have significantly improved the performance of CPA systems [8–10].

Optical pulses, whose temporal shape is parabolic, appear to be a very suitable candidate for reducing the impact of nonlinearities and to achieve high peak powers [8]. The use of parabolic pulses for fiber CPA has attracted considerable attention due to their ability to retain their intensity profile during propagation in highly nonlinear and dispersive media [11–13]. Self-phase modulation, which is proportional to the temporal intensity of the pulse, induces a linear frequency chirp during amplification of parabolic pulses. The linear chirp also allows efficient pulse compression, therefore making parabolic pulses especially suitable for use in a wide range of applications, such as high power femtosecond lasers, super-continuum generation for optical telecommunications, fiber amplifiers and chirped pulse amplification [14,15].

Several different approaches for parabolic pulse generation have been demonstrated. One of the earlier investigations in parabolic pulse generation was the theoretical demonstration of self-similar propagation of short pulses of parabolic intensity profile in optical fibers with normal group-velocity dispersion (GVD) and strong nonlinearity [13]. This concept has also been extended to optical fiber amplifiers, taking advantage of the asymptotic reshaping which occurs upon propagation within fiber amplifiers. By using the symmetry reduction technique,

parabolic pulses were shown to propagate self-similarly in a normal dispersion rare earth doped fiber amplifier [11,14,16]. Since then, much work has been done to generate parabolic pulses using dispersion-decreasing fiber (DDF) with normal group velocity dispersion [17,18], Raman amplification in optical fibers [19], and active or passive dispersion decreasing optical fibers [20]. Further investigations to passively generate parabolic pulses using tapered dispersion-decreasing fibers have also been reported [21,22].

The quality of the parabolic pulses generated with these approaches is only moderate, because the input pulses evolve asymptotically into a near parabolic shape. Also, as the pulses propagate, even as they retain their parabolic shape, their width and amplitude change, so there is not a well-defined mechanism to actively and dynamically control pulse characteristics. Also, it has been shown that third order dispersion and linear absorption have detrimental effects on parabolic pulse evolution and thus, on the performance of configurations utilizing DDF [23].

In this paper, a dynamic temporal pulse shaping technique is explored. Optical pulses from a mode-locked laser are temporally stretched to a duration of several nanoseconds. An intensity modulator is driven with an appropriate voltage signal to shape the input pulses into parabolic temporal profiles. This technique to generate a parabolic temporal intensity profile as well as dynamically control properties of the output pulse with any input pulse profile, is demonstrated experimentally.

2. Experimental setup

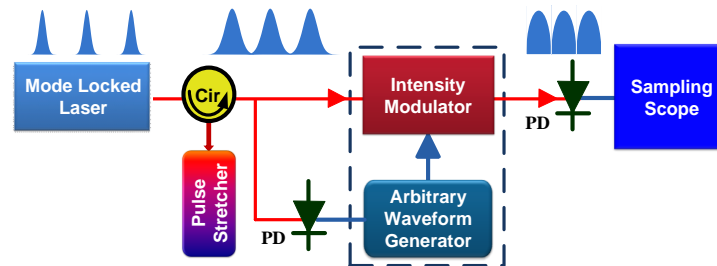


Fig. 1. Experimental setup for pulse shaping. Cir: circulator, PD: Photodiode.

The schematic for temporal pulse shaping is shown in Fig. 1. The near transform limited pulses generated by a mode-locked laser (MLL) are temporally stretched using dispersion-compensating fiber (DCF). Due to the high dispersion experienced by the pulses in the DCF, a wavelength-to-time mapping of the temporally stretched pulses is observed, so the temporal profile of the dispersed pulses closely resembles the shape of the input optical spectrum [24]. Subsequently, the stretched pulses are sent into an intensity modulator. A broad bandwidth arbitrary waveform generator (AWG) is used to generate a voltage drive signal. This drive signal is applied to the intensity modulator and is synchronized with the arrival of the stretched pulses, to impart a parabolic intensity profile to the stretched pulses.

To synchronize the voltage signals generated by the AWG with the incident optical pulses, pulses from the same mode-locked laser are photo-detected, and used to trigger the AWG. Since the quality of the shaped pulses directly depends on the quality of the voltage drive signal, an AWG with a sufficiently large bandwidth and high temporal resolution is required to generate a high quality drive signal. The AWG used in the experiment has a sampling rate of 10 GSamples/sec and a bandwidth of 10 GHz. After shaping, the parabolic pulses are photo-detected, and a sampling oscilloscope is used to monitor the quality of the pulses.

The typical transmission function of an intensity modulator is given by the equation

$$T(V) = \sin^2(\pi V / 2V_\pi) \quad (1)$$

where V is the applied voltage and V_π is the voltage at which the transmission of light through modulator changes from minimum to maximum. For a known intensity profile of an input pulse $I(t)_{\text{input}}$, the response function in time $P(t)$ of the intensity modulator required to generate a parabolic pulse can be calculated by:

$$P(t) = I(t)_{\text{output}} / I(t)_{\text{input}}, \quad (2)$$

where $I(t)_{\text{output}}$ is the desired output parabolic intensity profile.

From Eqs. (1) and (2), the required drive voltage signal can be obtained by:

$$V(t) = \arcsin \left(P(t)^{1/2} \right) 2V_\pi / \pi \quad (3)$$

The important aspect of this approach is that it allows dynamic control of the properties of the output pulses such as pulse shape, pulse width, and amplitude, and can be configured to work with input pulses with any intensity profile.

3. Results

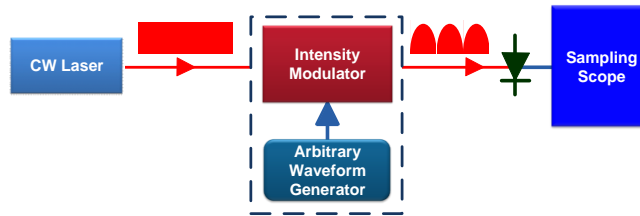


Fig. 2. Time domain parabolic pulse creation using a CW laser source.

Two different types of configurations were used in this work: a CW laser which simulates a square pulse input to the system and a MLL with Gaussian-shaped pulses. As a proof of concept experiment, a temporally gated CW laser is used as a seed source to simulate a square pulse input to the system, as can be seen in Fig. 2. It should be noted that the square pulses with linear chirp and uniform intensity can be produced with the frequency swept mode-locked laser [25].

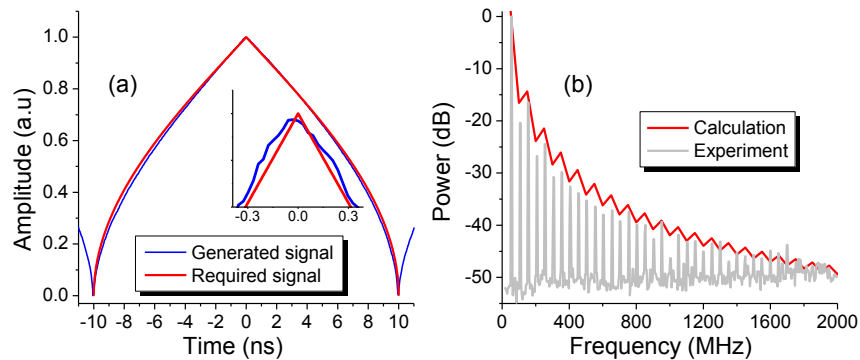


Fig. 3. (a) Required and generated drive signal for square input pulse; inset: zoom-in of the peak (b) Experimental and calculated power spectrum of drive signal.

Using the procedure described in section 2, the voltage drive signal is calculated and plotted in Fig. 3(a). It's evident that the drive signal (blue) generated by the AWG (Fig. 3(a)) matches very well with the required signal (red). The power spectrum of this signal is shown in Fig. 3(b), where the calculated power spectrum agrees with the measured spectrum up to

1.5 GHz. In this figure, the required power spectrum (red) is the envelope of the desired signal, because it is calculated from a non-periodic drive signal, unlike the measured power spectrum of periodic signals generated by the AWG (blue). The signal generated by the AWG is used to drive the modulator, resulting in parabolic pulses, plotted on a logarithmic scale in Fig. 4(a).

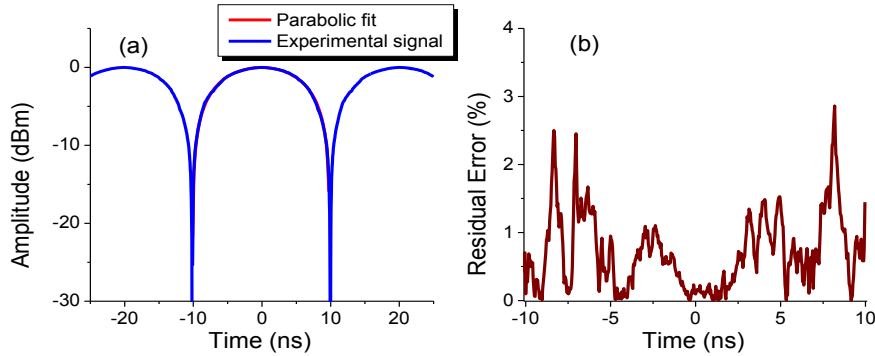


Fig. 4. (a) Sampling scope trace of output parabolic pulses (b) Residual error of generated parabolic pulse.

Notice that in Fig. 4(a), the pulse edges fall sharply following the parabolic fit, with an observed extinction ratio of 30 dB. To further demonstrate the precision of the generated parabola, the residual error over the full temporal duration of the pulse of 20 ns is calculated, by taking the difference of this parabolic pulse with the fitted parabola, and is shown to be less than 3%, as seen in Fig. 4(b).

In the second experiment, near transform limited pulses generated from a MLL are temporally stretched using 10 km of DCF. The shape of the optical spectrum is approximated by a Gaussian function with a full width at half maximum (FWHM) bandwidth of 6.6 nm, with a center wavelength at 1556 nm and a repetition rate of ~ 2.45 MHz. Pulses passing through the DCF are temporally stretched and spectrally dispersed, with the temporal profile of the dispersed pulses closely resembling the Gaussian shape of the optical spectrum. The DCF has a dispersion of ~ 1350 ps/nm which induces a linear frequency chirp and temporally stretches the pulses to 8.9 ns duration (FWHM): $\Delta t = D \cdot \Delta\omega$, where Δt is the pulse duration at FWHM, D is the dispersion of the DCF, and $\Delta\omega$ is the optical bandwidth (FWHM).

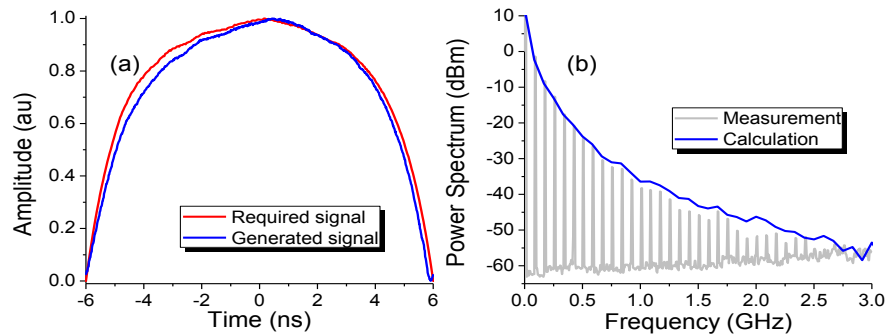


Fig. 5. (a) Drive signal for parabolic input pulse (b) Experimental and calculated power spectrum of drive signal.

Stretched pulses with longer temporal durations allow higher resolution shaping, due to the fixed temporal resolution of the AWG. The pulse train is then directed to an intensity modulator that is driven by an appropriate voltage signal, to produce pulses with parabolic

intensity profiles. Figure 5(a) shows the calculated drive signal, with a temporal duration of ~12 ns. The small discrepancies between the generated signal and the required signal are due to the bandwidth limitation of the AWG. The generated power spectrum of this drive signal can be seen in Fig. 5(b) and is found to be in agreement with the calculated power spectrum up to 1.75 GHz in bandwidth.

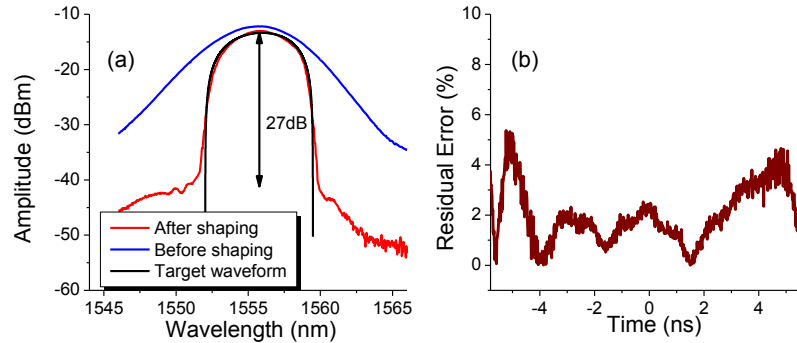


Fig. 6. (a) Optical spectrum before and after pulse shaping (b) Residual error of parabolic pulse.

The drive signal is applied to the intensity modulator and is synchronized with the arrival of the stretched pulses, resulting in parabolic pulses. Figure 6(a) shows the optical spectrum before and after pulse shaping, and an extinction ratio of 27 dB is observed. A close observation of Fig. 6(a) reveals that the optical power at the wings of the input pulse is attenuated to create parabolic shape at output pulse. The amplitude of pulses before and after pulse shaping has been adjusted for easy comparison. Figure 6(b) shows a residual error of less than ~5% over the pulse duration of 12 ns.

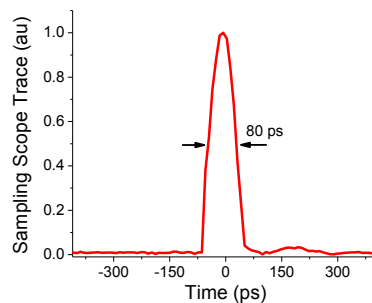


Fig. 7. Sampling oscilloscope trace of pulse after pulse shaping.

The pulses after shaping are compressed to achieve high peak power using a commercially available chirped fiber Bragg grating (CFBG) (Fig. 7). The parabolic pulses of 8 ns duration (FWHM) before compression are compressed to 80 ps. In this experiment, the limiting factor of compression appears to be the group delay ripple of the CFBG of approximately 80 ps. Using a different CFBG with smaller group delay ripple can reduce group delay ripple effect, and produce much shorter compressed pulses [7]. It should be noted that SPM phase can complicate compression of pulse. In our experiment, the peak power – length product is ~0.13 Wkm, which is much smaller than the 1.5 Wkm threshold in SMF for SPM, minimizing nonlinear residual dispersion.

4. Conclusion

A dynamic temporal approach for the generation of parabolic pulses which enables dynamic control of the pulse properties such as pulse shape, pulse width and amplitude has been investigated experimentally. Pulse shaping using a gated CW laser input is demonstrated, yielding parabolic pulses with less than 3% error and 30 dB signal to noise ratio. Using a mode-locked laser source, parabolic pulses with less than 5% error and 27 dB signal to noise ratio are achieved. These parabolic pulses are compressed by a factor of 100, using a chirped fiber Bragg grating. We believe this approach represents a significant step toward realizing high power CPA applications of fiber laser seeded systems.